High Optical Responsivity of InAlAs–InGaAs Metamorphic High-Electron Mobility Transistor on GaAs Substrate With Composite Channels

C.-S. Choi, *Student Member, IEEE*, H.-S. Kang, Woo-Young Choi, *Member, IEEE*, H.-J. Kim, W.-J. Choi, D.-H. Kim, K.-C. Jang, and K.-S. Seo

***Abstract*—The high optical responsivity of the InAlAs–InGaAs metamorphic high-electron mobility transistor on GaAs substrate with composite channels is reported. Experimental results verify that the photovoltaic effect causing the effective decrease of threshold voltage is responsible for the photoresponse to a 1.55-μm optical illumination.**

***Index Terms*—Metamorphic high-electron mobility transistor (HEMT), photodetector, phototransistor, responsivity.**

I. INTRODUCTION

THE photodetection characteristics of gallium–arsenide (GaAs)-based metal–semiconductor field-effect transistors and high-electron mobility transistors (HEMTs) have been extensively studied [1]–[3]. These three-terminal devices can provide high photocurrent gains without as much noise increment as in avalanche photodiodes and they make it possible to realize monolithic integration of photonic and microwave components on a single substrate. Recent works have been focused on the 1.3-μm photonic characteristics of indium–phosphide (InP)-based HEMTs for the development of integrated long-wavelength optical receivers [4], [5]. However, the low optical response of InP-based HEMTs under low optical incident power severely limits the sensitivity of the devices, thereby making it difficult to utilize these devices as a photodetector. In addition, low breakdown characteristics and difficulties in fabrication for InP-based HEMTs remain as obstacles for the integration with the other micro/millimeter-wave components.

In this letter, we fabricate the metamorphic InAlAs–InGaAs HEMT on a GaAs substrate with composite channels and investigate its photonic characteristics to 1.55-μm optical illumination. It is experimentally demonstrated that the metamorphic HEMT with the $In_{0.53}Ga_{0.47}As–In_{0.35}Ga_{0.65}As$ composite channels has very large optical responsivity at low incident optical power. The photodetection mechanism is clarified by investigating threshold voltage shifts in the HEMT under various incident optical powers.

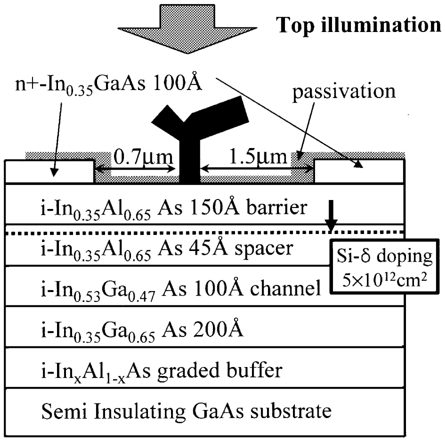

Fig. 1. Epitaxial structure of the InAlAs–InGaAs metamorphic HEMT on GaAs substrate with the composite channels.

II. DEVICE STRUCTURE AND EXPERIMENTAL SETUP

The metamorphic InAlAs–InGaAs HEMT was fabricated on the heterostructure epitaxial layers grown on a semi-insulating GaAs substrate by using molecular beam epitaxy. As shown in Fig. 1, epitaxial layers are made up of, from bottom to top, graded $In_xAl_{1-x}As$ buffers which were used to mitigate the lattice mismatch [6], composite channels with 20-nm $In_{0.35}Ga_{0.65}As$ and 10-nm $In_{0.53}Ga_{0.47}As$ layers, 4.5-nm $In_{0.35}Al_{0.65}As$ spacer with Si delta-doping (5×10^{12} cm^2), 15-nm $In_{0.35}Al_{0.65}As$ barrier, and 10-nm n$^+$ $In_{0.35}Ga_{0.65}As$ capping layer. The $In_{0.53}Ga_{0.47}As–In_{0.35}Ga_{0.65}As$ composite channels are used in order to improve carrier transport characteristics without sacrificing breakdown voltages for high power performance [6]. Hall measurements at room temperature showed that electron mobility and two-dimensional gas density are 2.3×10^{12}/cm^2 and 9370 cm^2/V·s, respectively.

The HEMT devices were fabricated with the standard processing steps. After the mesa isolation, ohmic contacts for the source–drain electrodes were made by Ni–Ge–Au alloys. The gate length and the width of the HEMT are 0.2 and 125 μm and the source-to-gate and the drain-to-gate separations are 0.7 and 1.5 μm, respectively. T-shaped Ti–Au gate was formed by using

---

Manuscript received October 28, 2002; revised February 28, 2003. This work was supported by the Ministry of Science and Technology of Korea through the National Research Laboratory Program.

C.-S. Choi, H.-S. Kang, and W.-Y. Choi are with the Department of Electrical and Electronic Engineering, Yonsei University, Seoul 120-749, Korea (e-mail: wchoi@yonsei.ac.kr).

H.-J. Kim was with the Nano-device Research Center, Korea Institute of Science and Technology, Seoul 136-792, Korea. He is now with the Korea Photonics Technology Institute, Gwangju 500-210, Korea.

W.-J. Choi is with the Nano-device Research Center, Korea Institute of Science and Technology, Seoul 136-792, Korea.

D.-H. Kim, K.-C. Jang, and K.-S. Seo are with the School of Electrical Engineering, Seoul National University, Seoul 151-742, Korea.

Digital Object Identifier 10.1109/LPT.2003.811339

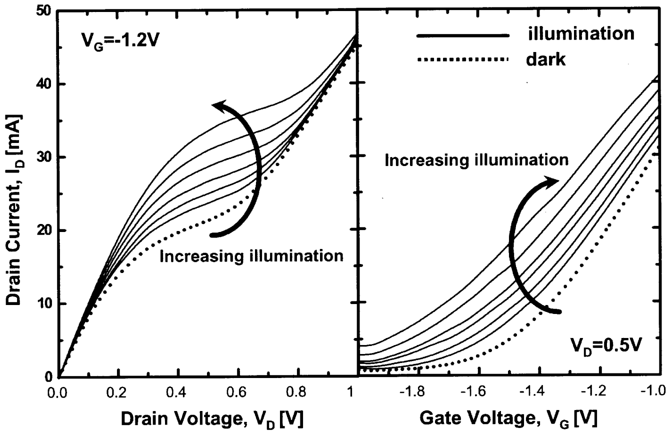

Fig. 2. Measured drain current (I_D) as a function of drain voltage (V_D) and gate voltage (V_G) under 1.55-μm optical illumination. The incident optical power increases from -12 to 3 dBm with a 3-dBm increment.

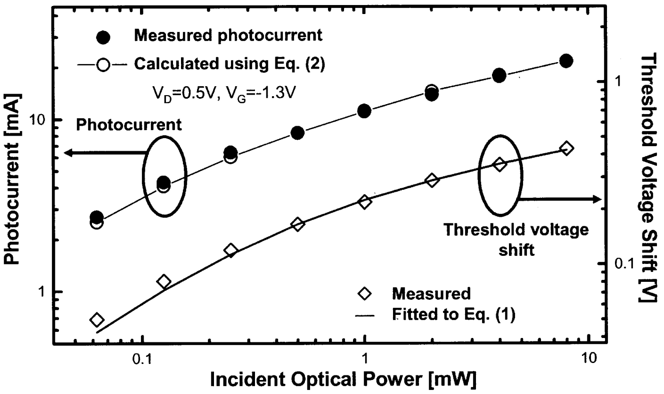

Fig. 3. Measured photocurrent (●) and the calculated increase in drain currents using (2) (-○-) as a function of incident optical powers (upper curve). The measured threshold voltage shift (◇) as a function of incident optical power; the line indicates the fitted data using (1) (lower curve). The gate bias condition of -1.3 V was only used in the measurement of increased drain currents.

E-beam lithography, evaporation, and liftoff process. Two-step gate recess processes were performed by wet-chemical etching using diluted citric and succinic acids. Finally, the silicon nitride was deposited for the passivation of the fabricated devices. The current gain cutoff frequency (f_T) and maximum oscillation frequency ($f_{\max}$) for the fabricated metamorphic HEMT are approximately 95 and 170 GHz under $V_G = 0.4$ V and $V_D = 1.0$ V, respectively.

The optical responses of the metamorphic HEMT were characterized with the semiconductor parameter analyzer (HP4145B) and a 1.55-μm distributed-feedback semiconductor laser diode. The device under test was illuminated by the light coming out of the cleaved single-mode fiber positioned just above the gate metal. It should be noted that the $\mathrm{In_{0.35}Al_{0.65}As}$ barrier and spacer layers are transparent to 1.55-μm lightwave, thus the absorption occurs at only 10-nm $\mathrm{In_{0.53}Ga_{0.47}As}$ channel. Because of the gate metal and the passivation layer, the actually absorbed optical power in the HEMT is estimated to be less than 10% of the incident optical power.

III. RESULTS AND DISCUSSION

Fig. 2 shows the measured I_D–V_D and I_D–V_G characteristics of the metamorphic HEMT for different incident optical powers. The solid lines represent drain currents under optical illumination and the dashed lines in the dark. The metamorphic HEMT exhibits significant increase in drain currents with increasing optical power, which varies from -12 to $+3$ dBm with a 3-dB increment measured at the output of the cleaved fiber. The major photodetection mechanism for the metamorphic HEMT is the photovoltaic effect which appears in the threshold voltage shifts of the I_D–V_G characteristics under optical illumination.

In order to fully investigate the influence of photovoltaic effect on the drain current of the HEMT, we measured threshold voltage shifts and photocurrents under different optical powers. Threshold voltages were extracted by extrapolating the linear region of I_D–V_G curves and finding the interception point on the V_G axis. Photocurrents were defined as $I_{\mathrm{Ph}} = I_D$ (illuminated) $-$ I_D (dark). The physical origin for photovoltaic effect in the InP-based HEMT can be explained as follows. When the absorption occurs in the $\mathrm{In_{0.53}Ga_{0.47}As}$ active channel, the photogenerated holes accumulate beneath the source region and effectively diminish the potential barrier between the source and the channel [6]. These optically induced barrier lowering effects result in the effective decrease of threshold voltages and the increase in drain currents. The threshold voltage shift caused by this photovoltaic effect can be expressed as

$$\Delta V_{TH} = \frac{A \cdot kT}{q} \ln\left(1 + \frac{B \cdot \tau_p \lambda P_{\mathrm{opt}}}{p \cdot hc}\right) \tag{1}$$

where kT/q is the thermal voltage, p is the intrinsic hole concentration, τ_P is the hole lifetime, hc/λ is the photon energy, A and B are the fitting parameters, and P_{opt} is the absorbed optical power.

In Fig. 3, threshold voltage (V_T) shifts for the illuminated HEMT are plotted as a function of incident optical powers. The ◇ points are measured data and the line is fitted according to (1). The well-fitted line indicates that V_T shift is attributed to the photovoltaic effect. The increase in drain currents caused by V_T shift is given by

$$\Delta I_D = G_m \Delta V_{TH} \tag{2}$$

where G_m is the intrinsic transconductance.

The • symbol in Fig. 3 indicates the measured photocurrent (I_{Ph}) at $V_D = 0.5$ V and $V_G = -1.3$ V. The -○- symbol and line are the additional drain current, predicted by (2) using measured V_T shifts and the intrinsic transconductance of 50.3 mS. From the result that the measured photocurrent coincides with the calculated increase in drain currents, we conclude that the major origin of photocurrents in the HEMT is the photovoltaic effect which causes the accumulation of optically generated holes at the source region to actually decrease the threshold voltage of the HEMT.

In the I_D–V_G characteristics shown in Fig. 2, it can be observed that photocurrents increase even when V_G is below the threshold voltage, which cannot be modeled by (2) as G_m is zero in this condition. The increase in subthreshold conduction currents in the illuminated HEMT is also due to the photovoltaic effects which reduce the potential barrier between the source and the channel [4].

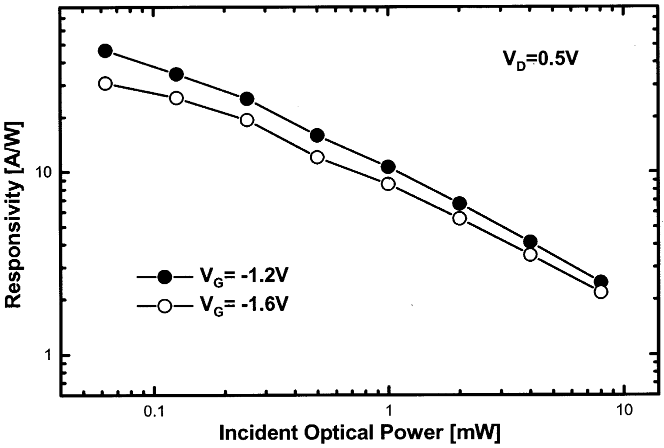

Fig. 4. Optical responsivities of the metamorphic HEMT as a function of incident optical powers under the condition of $V_G = -1.2$ and -1.6 V with $V_D = 0.5$ V.

It can be also observed that the photocurrents begin to decrease as the drain voltage increase over 0.8 V from the I_D–V_D characteristics shown in Fig. 2. This can be explained by the kink effects in InP-based HEMT [7]. As the accumulated holes generated by impact ionization enormously increase and cause kink currents at the high drain bias condition, photogenerated holes do not contribute to the threshold voltage shift.

The optical responsivities to 1.55-μm lightwave as a function of incident optical powers are shown in Fig. 4 with $V_G = -1.2$ V and $V_D = 0.5$ V. The responsivity is defined as the ratios between photocurrents and incident optical power at the output of the fiber. It is noted that the responsivity of the metamorphic HEMT with composite channels is much larger than that of any previously reported InP-based HEMTs in spite of high insertion loss at the illumination [4]. This is believed to arise from the optical absorption in only thin (10 nm) double heterojunction $In_{0.53}Ga_{0.47}As$ channel which effectively confines the photogenerated holes. However, further studies are required in order to clarify this. The high responsivity of 47 A/W is achieved at the incident input power of -12 dBm and it rapidly decreases with increasing incident optical power. Since the absorbed optical power in the channel is estimated to be less than 10% of incident optical power as mentioned above, the responsivity can be increased if more efficient optical coupling techniques are employed.

IV. CONCLUSION

The 1.55-μm optical response characteristics of the metamorphic HEMT with composite channels have been investigated. We observed the significant increase in drain currents under 1.55-μm optical illumination. Based on the experimental results, it was concluded that the photovoltaic effect caused by photogenerated excess holes in the source region is attributed to the predominant photodetection mechanism in the metamorphic HEMT. The experimental results also showed that the optical responsivity of the HEMT is strongly dependent on the incident optical power, and remarkably high responsivity of 47 A/W is obtained at -12-dBm incident optical power. Therefore, the metamorphic HEMT which has the high responsivity to 1.55-μm lightwave as well as the structural inherent advantages including high breakdown characteristics and availability of low cost GaAs substrates is expected to promise high optical gain phototransistors.

REFERENCES

[1] C. Y. Chen, A. Y. Cho, C. G. Bethea, P. A. Garbinski, Y. M. Pang, B. F. Levine, and K. Ogawa, "Ultrahigh speed modulation-doped heterostructure field effect photodetectors," *Appl. Phys. Lett.*, vol. 42, pp. 1040–1042, 1983.
[2] R. Simons and K. Bhasin, "Analysis of optically controlled microwave/millimeter-wave device structures," *IEEE Trans. Microwave Theory Tech.*, vol. 34, pp. 1349–1355, Dec. 1986.
[3] H. J. Kim, D. M. Kim, D. H. Woo, S. I. Kim, J. I. Lee, K. N. Kang, and K. Cho, "High photoresponsivity of a p-channel InGaP/GaAs/InGaAs double heterojunction pseudomorphic modulation-doped field effect transistor," *Appl. Phys. Lett.*, vol. 72, pp. 584–586, 1998.
[4] Y. Takanashi, K. Takahata, and Y. Muramoto, "Characteristics of InAlAl–InGaAs high-electron-mobility transistors under illumination with modulated light," *IEEE Trans. Electron Devices*, vol. 46, pp. 2271–2277, Dec. 1999.
[5] C. Rauscher and K. J. Williams, "Heterodyne reception of millimeterwave-modulated optical signals with a InP-based transistor," *IEEE Trans. Microwave Theory Tech.*, vol. 42, pp. 2027–2034, Nov. 1994.
[6] M. Chertouk, H. Heiss, D. Xu, S. Kraus, W. Klein, G. Bohm, G. Trankle, and G. Weimann, "Metamorphic InAlAs–InGaAs HEMTs on GaAs substrate with a novel composite channels design," *IEEE Electron Device Lett.*, vol. 17, pp. 273–275, June 1996.
[7] M. H. Somerville, A. Ernst, and J. A. del Alamo, "A physical model for the kink effect in InAlAs–InGaAs HEMTs," *IEEE Trans. Electron Devices*, vol. 47, pp. 922–930, May 2000.